^{68}Ga-DOTATOC PET/CT of Neuroendocrine Tumors: Spotlight on the CT Phases of a Triple-Phase Protocol

Juri Ruf[*1,2], Jan Schiefer[*1], Christian Furth[1], Ortud Kosiek[1], Siegfried Kropf[3], Friederike Heuck[4], Timm Denecke[2], Marianne Pavel[4], Andreas Pascher[5], Bertram Wiedenmann[4], and Holger Amthauer[1,2]

[1]Klinik für Radiologie und Nuklearmedizin, Universitätsklinikum Magdeburg A.ö.R., Magdeburg, Germany; [2]Klinik für Strahlenheilkunde, Campus Virchow-Klinikum, Charité-Universitätsmedizin Berlin, Berlin, Germany; [3]Institut für Biometrie und Medizinische Informatik, Medizinische Fakultät der Otto-von-Guericke-Universität, Magdeburg, Germany; [4]Medizinische Klinik m. S. Hepatologie und Gastroenterologie, Campus Virchow-Klinikum, Charité-Universitätsmedizin Berlin, Berlin, Germany; and [5]Klinik für Allgemein-, Viszeral- und Transplantationschirurgie, Campus Virchow-Klinikum, Charité-Universitätsmedizin Berlin, Berlin, Germany

The diagnostic value of neuroendocrine tumor (NET) imaging using PET with integrated CT is dependent on both components. This retrospective study assessed the value of the single CT phases of a triple-phase (early arterial, portal-venous inflow, and venous) CT protocol in comparison to ^{68}Ga-DOTATOC PET in a masked reading. **Methods:** ^{68}Ga-DOTATOC PET/CT examinations from 51 patients with known or suspected NET were included. Two readers assessed the data of PET and each of the 3 CT phases for NET lesions independently (using a 3-point score: 1 = benign, 2 = indeterminate, and 3 = malignant) and by consensus (using binary benign/malignant interpretation only). Only lesions within the field of the abdominal scan were evaluated. Clinical and imaging follow-up, histopathology (if available), and the decision of an interdisciplinary truth-panel served as a standard of reference. In addition to the calculation of standard statistical parameters (including general linear mixed models), interobserver reliability was estimated (Cohen's κ). **Results:** Of 510 abdominal lesions observed, 354 were classified as malignant. Sensitivity was 77.1% for combined triple-phase CT, 53.4% for arterial CT, 66.1% for portal-venous CT, 66.9% for venous CT, and 72.8% for PET. The respective specificities were 85.3%, 92.9%, 92.3%, 89.7%, and 97.4%, and the respective accuracies were 79.6%, 65.5%, 74.1%, 73.9%, and 80.4%. Although arterial CT was found to be inferior to PET, portal-venous CT, and venous CT ($P < 0.001$), the differences between the other scans were not significant. Detection was exclusively by PET for 16.1% of lesions, by triple-phase CT for 20.3%, by arterial CT for 0.5%, by portal-venous CT for 3.9%, and by venous CT for 3.9%. Regarding interobserver reliability, the κ-value was 0.768 for PET, 0.391 for triple-phase CT, 0.577 for arterial CT, 0.583 for portal-venous CT, and 0.482 for venous CT. **Conclusion:** No CT phase can be omitted in NET imaging, and the triple-phase protocol continues to be strongly recommended also for PET/CT.

Key Words: neuroendocrine tumor; NET; ^{68}Ga-DOTATOC; PET/CT; multiphase CT protocol

J Nucl Med 2011; 52:697–704
DOI: 10.2967/jnumed.110.083741

Neuroendocrine tumors (NETs) are a heterogeneous group of rare neoplasms derived from cells of the neuroendocrine system with varying malignant potential. Aside from the expression of common neural markers, NETs synthesize a variety of active mediators, optionally leading to characteristic endocrine syndromes. Diagnosis frequently occurs late because of unspecific symptoms and less frequently occurs on the manifestation of endocrine symptoms related to metastatic disease (*1–3*). Moreover, in midgut NET the primary tumor is often small and difficult to detect (*4,5*).

Overexpression of somatostatin receptors (SSTRs), especially subtype 2, is a special feature of most NETs (*6*), making functional imaging by radiolabeled somatostatin analogs possible either with conventional scintigraphy or with PET. In comparison to tracers such as ^{111}In-DTPA-octreotide for conventional scintigraphy (*7*), PET ligands such as ^{68}Ga-DOTATOC have been shown to be especially useful when combined with integrated CT (*8–10*).

Recently, our group reported a change in therapy management for 38% of all NET patients due to the additional use of hybrid ^{68}Ga-DOTATOC PET/CT. Moreover, the synergistic value of PET and combined multiphase CT in clinical decision making was demonstrated, since about one third of all lesions were detected by only one of the submodalities alone (*11*).

Although the usefulness of multiphase CT protocols for hepatic NET metastases was first reported as early as 1998 (*12*), and the European Neuroendocrine Tumor Society also recently recommended the use of such protocols (*13*), analyses of the value of the single phases alone have been published only rarely.

Received Sep. 29, 2010; revision accepted Jan. 31, 2011.
For correspondence or reprints contact: Juri Ruf, Klinik für Radiologie und Nuklearmedizin, Universitätsklinikum Magdeburg A.ö.R, Leipziger Strasse 44, 39120 Magdeburg, Germany.
E-mail: juri.ruf@med.ovgu.de
*Contributed equally to this work.

To our knowledge, only one study is available on somatostatin receptor PET/CT. That study reported a great variance in NET lesion detection, depending not only on the CT phase but also on the lesion type (organ, bone, lymph node) and CT mode (diagnostic vs. low-dose CT) (*14*). However, as that study protocol did not include an early portal-venous phase, the aim of the present investigation was to assess the value of the early arterial, portal-venous inflow, and venous CT phases in comparison to PET in NET patients examined with ^{68}Ga-DOTATOC PET/CT.

MATERIALS AND METHODS

Patients

Image data of 51 consecutive patients (25 men and 26 women; mean age, 57 ± 13 y; range, 31–79 y) with known or suspected NET, who had undergone triple-phase contrast-enhanced ^{68}Ga-DOTATOC PET/CT between June 2006 and July 2008 at the Charité–University Hospital/Berlin, were retrospectively reevaluated in a blinded reading. All patients had been under the care of the institutional interdisciplinary NET tumor board. Patients with known secondary malignancy or intolerance of iodine contrast medium were excluded from the analysis. Indications for the PET/CT examination had been clinical suspicion of NET (n = 1), a search for the primary tumor in the case of neuroendocrine carcinoma of unknown primary (n = 17), staging of known NET disease (n = 9), and restaging or suspected recurrence (n = 24).

Therapy with long-acting depot somatostatin analogs had been stopped 4 wk before the examination in 4 patients. In no patient had a switch to short-lived somatostatin analogs been necessary (*7*).

All patients provided written consent to the examination and the evaluation of their data. This retrospective study was approved by the institutional ethics committee.

PET/CT Protocol

Imaging had been performed with a dedicated 16-slice PET/CT scanner (Biograph 16; Siemens Healthcare AG). A whole-body PET scan (base of skull to groin) and a triple-phase intravenous contrast-enhanced CT scan were obtained.

The PET scans were acquired at 5 or 6 bed positions (3 min each) 1 h after intravenous administration of 100–120 MBq of ^{68}Ga-DOTATOC, prepared according to the method of Zhernosekov et al. (*15*).

PET images derived from a 168 × 168 acquisition matrix were iteratively reconstructed with scatter correction using ordered-subset expectation maximization (5 iterations; 8 subsets). An attenuation map (μ-map) generated from the whole-body venous CT scan was used for attenuation correction.

Triple-phase CT was based on a protocol used for liver imaging (*16*). One hundred milliliters of nonionic iodinated contrast agent (iopromide [Ultravist 370]; Bayer Schering Pharma) were administered at a flow rate of 4 mL/s followed by a saline flush (40 mL; 4 mL/s). Triple-phase CT (automatic tube current modulation with maximum tube current, 230 mAs; tube voltage, 120 kV; gantry rotation, 0.5 s) was performed using bolus tracking. The early arterial phase (scan initiation 5 s after reaching the 100-Hounsfield-unit threshold in the abdominal aorta, resulting in a delay of ~25 s) and the portal-venous inflow phase (20-s delay from the beginning of the arterial phase) covered the upper abdomen. The venous phase (50-s delay from the arterial phase) was performed as whole-body CT (head to thigh). Detector collimation was 16 × 0.75 mm for arterial CT and 16 × 1.5 mm for venous CT. Primary image reconstruction was performed at a 0.75- and 4-mm slice thickness for arterial CT and a 2- and 5-mm slice thickness for venous CT (increment, 0.5 mm). Patients were positioned supine with their arms elevated.

Because of the potential for attenuation correction artifacts, no positive oral contrast medium was included in this protocol (*17,18*) and negative oral contrast medium was used infrequently.

Interpretation of Findings

A blinded reading was performed by 2 independent observers. The 51 datasets, consisting of the 3 phases of the CT scan and the attenuation-corrected PET scan, were read in random order on a dedicated PET/CT workstation (Leonardo workstation with e.soft 4 software; Siemens Healthcare AG). Both readers (4 and 8 y of experience in anatometabolic NET imaging) had been trained using sample files (5 full datasets) before study initiation.

Each subscan was read separately and assessed for nonphysiologic findings classified as lesions (the CT phases were read separately and as a combined triple-phase scan). Only lesions within the area of the abdominal triple-phase CT scan were considered in this study. Images were evaluated in coronal, axial, and sagittal planes. For the topographic assignment of lesions in the PET scan, image fusion with the venous CT component served as a reference. Lesions were categorized by anatomic location (liver, pancreas, intestinal tract, lymph node, bone, basal lung, and other) and interpreted by each reader using a 3-point score (1 = benign, 2 = indeterminate, and 3 = malignant).

All lesions in a given subscan were first interpreted individually (for interobserver analysis) and then by consensus using a binary ranking system only (i.e., benign vs. malignant). If no consensus could be reached, a third reader determined the definitive classification.

When tumor-suggestive lesions were found on CT images, the following criteria served for further characterization: shape, delineation from surrounding tissue, internal structure, density, and contrast enhancement. Indicators of malignant infiltration of lymph nodes were diameter perpendicular to longest axis exceeding 1.5 cm, suggestive contrast enhancement, and a spheric configuration (length-to-thickness ratio < 2). Groups of multiple enlarged lymph nodes in one location not matching the size criteria were also classified as tumor lesions. Gastrointestinal lesions were rated as malignant if focal wall thickening, intraluminal polypoid growth, hyperperfusion, or desmoplastic mesenteric reactions were present. Single pulmonary nodules with a diameter exceeding 5 mm or a suggestive configuration (e.g., spicular) were classified as metastases if they did not show any sign of a benign origin (e.g., pattern of calcification). Groups or multiple scatterings of pulmonary nodules were classified as malignant if they suggested metastatic disease. All bone lesions—osteoblastic, osteolytic, and mixed—visually suggestive of metastatic disease (e.g., from configuration, size, soft-tissue components, or bone marrow infiltration) were considered to be malignant.

PET findings showing significantly increased focal tracer uptake, based on visual assessment, were classified as malignant. Regions with physiologically increased tracer uptake (e.g., spleen, adrenal gland, pituitary gland, or uncinate process of the pancreas) or organ systems involved in tracer elimination (liver, kidney, urinary tract) were not subjected to rating if they presented typical patterns of physiologic uptake (*8*).

Because patients with a known secondary malignancy had been excluded from the analysis, all findings suggestive of malignancy were attributed to NET disease.

Reference Standard

Although any cyto- or histopathologic specimens and surgical reports available were considered for assessment of the lesions, it was neither practically nor ethically feasible to establish a true histopathology-based gold standard for all lesions. Thus, a surrogate reference standard had to be created for the lesions, based on the clinical and imaging follow-up (mean, 21.2 mo; range, 12–36 mo) performed by the NET Center of the Department of Gastroenterology. Furthermore, all available clinical, laboratory, and imaging data (follow-up CT, PET/CT, MRI, ultrasonography, endosonography, and conventional somatostatin receptor scintigraphy) had been assessed by an interdisciplinary truth-panel (consisting of an endocrinologist with oncologic expertise, a gastroenterologist, an abdominal surgeon, a radiologist, and a nuclear medicine specialist).

Statistical Analyses

The sensitivity and specificity of the 3 CT phases and the PET scans for NET lesion detection were determined for both the patient-based and the lesion-based analyses by comparing the result of the consensus interpretation with the reference standard. Moreover, accuracy was calculated for the lesion-based analysis. In addition, percentages for exclusive detection by a specific subscan (i.e., single CT phases and PET) were determined.

For comparison of the methods (i.e., subscans), generalized linear mixed models (SAS, PROC GLIMMIX) were used for the binary outcome variables, with the methods as fixed factors and patients and their lesions as random factors. To test for different ratings in individual subscans, the mean ratings were compared, again using linear mixed models (SAS, PROC MIXED). The Tukey–Kramer method was used to adjust for multiple testing.

In contrast to these analyses, interobserver reliability was calculated from the individual reader 3-point-score interpretations using Cohen's κ, which was interpreted according to the method of Landis and Koch: $\kappa < 0$, poor; $\kappa = 0$–0.2, slight; $\kappa = 0.2$–0.4, fair; $\kappa = 0.4$–0.6, moderate; $\kappa = 0.6$–0.8, substantial; $\kappa = 0.9$–1.0, almost perfect (*19*). For all tests, a P value of less than 0.05 was considered statistically significant. All statistical analyses were performed using SPSS Statistics 17.0 software (SPSS Inc.) and SAS 9.2 (SAS Institute Inc.).

RESULTS

Patients and Lesions

According to the reference standard, the primary tumor was located in the gut for 16 patients, the pancreas for 13, the bronchial system for 4, and the colon or rectum for 3. One patient had a multifocal gastroenteropancreatic primary. In the remaining 14 patients, the site of the primary remained unknown.

In the 51 PET/CT examinations, a total of 510 lesions were detected in the abdominal range of the triple-phase CT scan (320 visualized by PET and 457 by CT). The mean size of lesions measurable on CT was 1.8 ± 1.2 cm (range, 0.5–10.3 cm).

Patient-Based Analysis

By our reference standard, 39 of 51 patients had NET disease at the time of examination. Of these 39, 32 (82.1%) were correctly identified by PET, 33 (84.6%) by triple-phase CT, 27 (69.2%) by arterial CT, 31 (79.5%) by portal-venous CT, and 31 (79.5%) by venous CT.

Of the 12 tumor-free patients, 8 (66.7%) were correctly identified by PET, 6 (50.0%) by triple-phase CT, 7 (58.3%) by arterial CT, and 8 (66.7%) by venous CT and portal-venous CT.

Hepatic manifestation was apparent in 24 patients. Of these, 19 (79.2%) were identified by PET, 21 (87.5%) by triple-phase CT, 15 (62.5%) by arterial CT, 21 (87.5%) by portal-venous CT, and 19 (79.2%) by venous CT. Lymph node metastases were manifested in 23 patients. Of these, 19 (82.6%) were classified correctly by PET, 15 (65.2%) by triple-phase CT, 13 (56.5%) by portal-venous CT, 14 (60.9%) by arterial CT, and 14 (60.9%) by venous CT. Of the 3 patients with bone metastases, 1 was identified by PET and 2 by triple-phase CT (with no differences between CT subscans). Of the 15 patients with a pancreatic primary or metastases, 14 (93.3%) were correctly identified by PET, 9 (60.0%) by triple-phase CT, and 8 each (53.3%) by arterial CT, portal-venous CT, and venous CT. Gastrointestinal manifestations in 2 patients were exclusively detected by PET. Only 1 of the 4 patients with pulmonary manifestations could be identified by PET, whereas all 4 were identified by triple-phase CT or venous CT alone. Separate arterial CT and portal-venous CT scans each identified only 2 of the 4. Five patients had manifestations in other places. Of these, 4 were classified correctly by PET, 3 by triple-phase CT, and 3 by each of the subscans.

Lesion-Based Analysis

In the lesion-based analysis, malignancy was attributed to 354 (69.4%) of the 510 lesions (Table 1); 77.1% of all malignant lesions were detected by triple-phase CT and 72.8% by PET. Of all malignant lesions, 53.4% were detected on arterial CT, 66.1% on portal-venous CT, and 66.9% on venous CT. No significant differences in sensitivity were observed on comparison of triple-phase CT and PET ($P = 0.1715$). Nor were any significant differences in sensitivity revealed when portal-venous CT, venous CT, and PET were compared with one another, whereas arterial CT was found to be significantly less sensitive than the other subscans ($P < 0.001$). Specificities were 97.4% for PET

TABLE 1
Anatomic Distribution of Lesions

Lesions	Liver	Lymph node	Bone	Pancreas	Gastrointestinal tract	Basal lung	Other	Total
All (*n*)	313 (61.3%)	107 (21.0%)	31 (6.1%)	32 (6.3%)	4 (0.8%)	9 (1.8%)	14 (2.8%)	510 (100%)
Malignant (*n*)	242 (68.4%)	58 (16.4%)	23 (6.9%)	17 (4.8%)	2 (0.6%)	6 (1.7%)	6 (1.7%)	354 (100%)

and 85.3% for triple-phase CT (arterial CT, 92.9%; portal-venous CT, 92.3%; venous CT, 89.7%), with no significant differences ($P = 0.2573–0.9790$). Accuracy was 80.4% for PET, 79.6% for triple-phase CT, 65.5% for arterial CT, 74.1% for portal-venous CT, and 73.9% for venous CT. PET was significantly superior to combined and single CT phases ($P = 0.001–0.0308$).

On subdividing the patients into those who had received systemic therapy ($n = 17$)—for example, chemotherapy, interferon, or somatostatin analogs—and those who were naïve to systemic therapy ($n = 34$), we observed no significant differences between the groups ($P = 0.2959$).

An exclusive detection of malignant lesions was observed in 16.1% by PET and 20.3% by triple-phase CT (0.5% only by arterial CT, 3.9% only by portal-venous CT, and 3.9% only by venous CT).

The sensitivity of triple-phase CT for the detection of liver metastases ($n = 242$) was significantly better than that of PET (84.7% vs. 78.5%; $P = 0.0495$). In contrast, PET performed significantly better than arterial CT (53.7%; $P < 0.001$), but not significantly better than portal-venous CT (72.3%, $P = 0.1265$) or venous CT (70.7%; $P = 0.1852$) (Fig. 1). Whereas arterial CT had the lowest sensitivity of all CT phases ($P < 0.001$), the differences between portal-venous CT and venous CT were insignificant ($P = 0.9987$). The specificities for hepatic lesions were 98.6% for PET, 78.9% for triple-phase CT, 87.3% for arterial CT, 89.8% for portal-venous CT, and 85.7% for venous CT. As a result, the most accurate modality was PET, and PET was significantly better than CT ($P = 0.001–0.0177$), with the exception of portal-venous CT ($P = 0.1252$).

More than 25% of all malignant liver lesions were seen either only on PET (10.3%) or only on CT (16.5%). With regard to CT, each subscan, including arterial CT, provided additional information (arterial CT, 0.4%; portal-venous CT, 5.8%; and venous CT, 4.1%).

The highest sensitivity for lymph node metastasis detection ($n = 58$; Fig. 2) was reached by PET (67.2%), followed by triple-phase CT (56.9%), venous CT (55.2%), and arterial and portal-venous CT (48.3% each), though neither difference was significant ($P = 0.0.2770–0.8529$). About 45% of all lymph node metastases were detected exclusively by PET (27.5%) or triple-phase CT (17.2%). Concerning CT, 1.7% of all metastases were exclusively detected by arterial CT and 3.4% by venous CT. No additional malignant lesions were detected by portal-venous CT. The specificities for lymph node metastases were 100% for PET, 85.7% for triple-phase CT, 95.9% for arterial CT, 89.8% for portal-venous CT, and 85.7% for venous CT. The accuracy was 82.2% for PET, 70.1% for triple-phase CT, 70.1% for arterial CT, 67.3% for portal-venous CT, and 69.2% for venous CT. PET was significantly more accurate than portal-venous CT ($P = 0.0204$).

Sensitivity for bone metastases ($n = 23$) was higher on CT (69.6% for triple-phase CT and the CT subscans) than on PET (21.7%), with CT detecting significantly more bone metastases than PET ($P = 0.0052$). In contrast, specificity for both CT and PET was 100%. Exclusive detection of a bone lesion was seen in 21.7% by PET and 69.5% by CT, with no difference between the single CT subscans alone.

Almost all malignant pancreas lesions ($n = 17$) were detected by PET (94.1%), whereas triple-phase CT detected only about half of the lesions (triple-phase CT, 58.8%; subscans, 52.9% each), thus showing PET to be superior to CT (triple-phase CT, $P = 0.0500$; CT subscans, $P = 0.0427$ each). Specificities were 80.0% for PET and 100% for all CT scans. An exclusive lesion detection was seen for approximately 46.9% of all pancreatic lesions: 41.1% were detected only by PET, 5.8% only by triple-phase CT, and none only by a single CT scan.

Lesions within the gastrointestinal tract ($n = 2$) were detected by PET only.

All malignant basal lung metastases ($n = 6$) were detected by triple-phase CT (arterial CT and portal-venous CT, 50.0%; venous CT, 100%), whereas PET detected only 16.7%. The specificities were 100% for arterial CT, portal-venous CT, and PET and 66.7% for venous CT and triple-phase CT. Of the basal lung lesions, 83.3% were detected exclusively by CT and none by PET.

The sensitivity for other lesions ($n = 6$) was 83.3% for PET and 50.0% for all CT scans, with a specificity of 100% for all submodalities.

Of these lesions, 33.3% were exclusively detected by triple-phase CT or PET.

A full list of sensitivity, specificity, and accuracy values is shown in Table 2 and Supplemental Table 1 (supplemental materials are available online only at http://jnm.snmjournals.org).

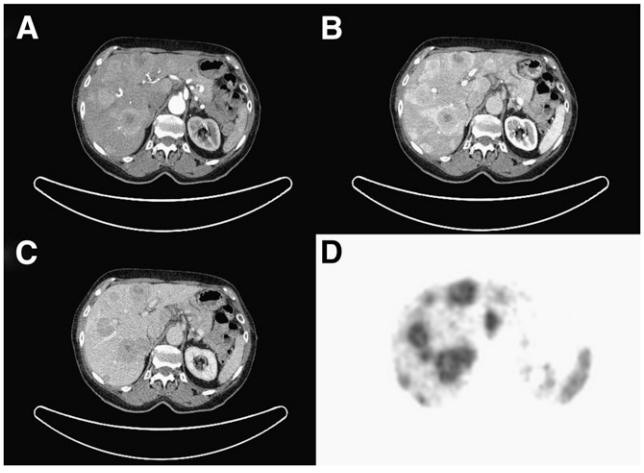

FIGURE 1. A 78-y-old woman with multiple hepatic metastases of pancreatic NET most visible on portal-venous CT (B) and PET (D). In contrast, some lesions were only barely visible on arterial CT (A) and venous CT (C). After ^{68}Ga-DOTATOC PET/CT, patient was referred for chemotherapy (streptozotocin/5-fluorouracil) because of progressive disease.

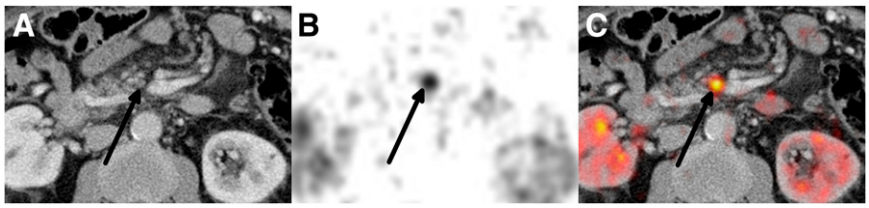

FIGURE 2. Small mesenteric lymph node metastasis (arrows) of pancreatic NET in 71-y-old man: portal-venous CT (A), ^{68}Ga-DOTATOC PET (B), and fused PET/CT (C). Not meeting CT malignancy criteria, with diameter of 0.55 cm perpendicular to longest axis and round configuration, this lesion was detected only because of increased uptake on PET.

Rating Differences Between Subscans

In the 3-point rating system, differences in lesions between triple-phase CT and PET were significant ($P = 0.003$). Also, findings from arterial CT were rated differently from all other CT subscans and PET ($P < 0.001$). This was especially true for liver lesions ($P < 0.001$). Differing ratings were revealed for liver lesions, on comparison of PET and triple-phase CT ($P = 0.008$) or PET and portal-venous CT ($P = 0.033$). No difference in general rating was found between portal-venous CT and venous CT ($P = 0.740$) or between venous CT and PET ($P = 0.317$). There was a significant difference in the ratings attributed to lymph node lesions on arterial CT and PET ($P = 0.017$), whereas comparisons of all other scans, including triple-phase CT, with one another failed to reveal any significantly different ratings. All CT scans of bone and pancreatic lesions were rated differently from PET ($P < 0.001$), with no significantly different ratings between single CT subscans. Gastrointestinal lesions outside liver and pancreas were not rated significantly differently in any particular scan. Different ratings were attributed to basal lung lesions on triple-phase CT ($P < 0.001$) or venous CT compared with PET ($P = 0.001$). Lesions in other locations were rated differently from PET on triple-phase CT ($P = 0.028$) and on arterial CT and portal-venous CT ($P = 0.016$ each).

Interobserver Reliability

Interobserver reliability was substantial for PET ($\kappa = 0.768$), fair for triple-phase CT ($\kappa = 0.391$), and moderate for arterial CT ($\kappa = 0.577$), portal-venous CT ($\kappa = 0.583$), and venous CT ($\kappa = 0.482$).

A full list of interobserver agreement and κ-values according to the different anatomic locations is presented in Table 3.

Triple-phase CT showed moderate agreement for bone and basal lung lesions; fair agreement for liver, lymph node, and pancreas lesions; and slight agreement for other lesions. Arterial CT showed substantial agreement for basal lung, liver, and bone lesions, whereas on portal-venous CT substantial agreement for liver and bone lesions was observed. In contrast, only fair to moderate agreement was reached for lymph node, pancreas, and other lesions in these 2 phases. Moderate agreement was reached for liver, basal lung, and bone lesions on venous CT and fair agreement for lymph node and pancreas lesions. PET showed almost perfect or substantial agreement for all except those classified as other lesions.

Concerning the different CT subscans, liver and basal lung lesions were rated more concordantly on arterial CT than on any other CT phase. Pancreatic lesions were rated more concordantly on arterial CT and portal-venous CT than on venous CT.

DISCUSSION

The value of SSTR imaging was greatly enhanced by the introduction of PET tracers such as ^{68}Ga-DOTATOC, especially when used in a PET/CT setting. Although recent studies (*8–10*) have emphasized the value of PET, an optimization of CT protocols for maximum synergy with PET is also highly desirable. In analogy to a previous report by our group (*11*), the present data demonstrate that a remarkable number of NET lesions would be missed by single-modality imaging alone and that the high sensitivity of hybrid SSTR PET/CT stems from the combined use of PET and multiphase CT. Although a consensus meeting of experts in the field of NET recently led to the publication of a recommendation to use multiphase CT for imaging of NET (*13*), data on the value of the different single CT phases are heterogeneous and scarce (*14,20,21*). For protocol simplification and a potential reduction of exposure to radiation (*22*), clarity on whether a certain contrast phase is definitely inferior and could potentially be omitted would be most desirable.

Reports on the sensitivities of individual CT phases for lesions other than liver are scarce. With respect to overall lesion detection by arterial CT, we found, at 53.4%, a slightly lower sensitivity than the 59% reported by Wieder et al. (*20*)

Concerning hepatic metastases, however, our sensitivities of 53.7% for arterial CT and 70.7% for venous CT confirm the results of earlier studies (*14*). Nevertheless, the sensitivity of arterial CT for liver metastases was rather low, and both portal-venous CT and venous CT performed significantly better ($P < 0.001$).

A possible reason for this unexpectedly poor performance of arterial CT may be the heterogeneous study population examined, with indications ranging from primary diagnosis to restaging after several lines of therapy. Although no statistical differences have been observed overall between patients with and without prior systemic therapy, it is still conceivable that alterations in tumor vascularity, such as those due to interferon or somatostatin analog treatment (*23–25*), or washout effects in later scan

TABLE 2
Sensitivity, Specificity, and Accuracy of Lesion-Based Analysis According to Anatomic Location and Submodality

Location	CT phase				PET
	Combined CT	Arterial CT	Portal-venous CT	Venous CT	
All (n = 354)					
Sensitivity	77.1%	53.4%	66.1%	66.9%	72.8%
Specificity	85.3%	92.9%	92.3%	89.7%	97.4%
Accuracy	79.6%	65.5%	74.1%	73.9%	80.4%
Liver (n = 242)					
Sensitivity	84.7%	53.7%	72.3%	70.7%	78.5%
Specificity	78.9%	87.3%	90.1%	88.7%	98.6%
Accuracy	73.8%	61.3%	76.4%	74.8%	83.1%
Lymph node (n = 58)					
Sensitivity	56.9%	48.3%	48.3%	55.2%	67.2%
Specificity	85.7%	95.9%	89.8%	85.7%	100.0%
Accuracy	70.1%	70.1%	67.3%	69.2%	82.2%
Bone* (n = 23)					
Sensitivity	69.6%	69.6%	69.6%	69.6%	21.7%
Specificity	100.0%	100.0%	100.0%	100.0%	100.0%
Accuracy	77.4%	77.4%	77.4%	77.4%	41.9%
Pancreas* (n = 17)					
Sensitivity	58.8%	52.9%	52.9%	52.9%	94.1%
Specificity	100.0%	100.0%	100.0%	00.0%	80.0%
Accuracy	78.1%	75.0%	75.0%	75.0%	87.5%
Gastrointestinal tract* (n = 2)					
Sensitivity	0.0%	0.0%	0.0%	0.0%	100.0%
Specificity	100.0%	100.0%	00.0%	100.0%	100.0%
Accuracy	50.0%	50.0%	50.0%	50.0%	100.0%
Basal lung* (n = 6)					
Sensitivity	100.0%	50.0%	50.0%	100.0%	16.7%
Specificity	66.7%	100.0%	100.0%	66.7%	100.0%
Accuracy	88.9%	66.7%	66.7%	88.9%	44.4%
Other* (n = 6)					
Sensitivity	50.0%	50.0%	50.0%	50.0%	83.3%
Specificity	100.0%	100.0%	100.0%	100.0%	100.0%
Accuracy	66.7%	66.7%	66.7%	66.7%	78.6%

*Low lesion count; cautious interpretation recommended.

phases could influence image quality. Although we consider the 100 mL of contrast agent applied to be sufficient for the 60- to 90-kg patient weight encountered in our collective, it must be acknowledged that arterial enhancement, in particular, will be inferior in larger patients with a correspondingly larger distribution volume. To compensate for this potential bias, a rather high injection rate is chosen, producing a high attenuation peak that can be reliably visualized. However, the short injection rate in turn increases the risk that the peak attenuation is missed. Fur-

TABLE 3
Interobserver Reliability: Cohen's κ-Values for Different Submodalities and Anatomic Locations

Location	CT phase				PET
	Combined CT	Arterial CT	Portal-venous CT	Venous CT	
Liver	0.375	0.715	0.675	0.560	0.777
Lymph node	0.306	0.268	0.342	0.345	0.720
Bone	0.495	0.811	0.811	0.495	0.890
Pancreas	0.329	0.411	0.494	0.296	0.723
Gastrointestinal tract	NA	NA	NA	NA	1.000
Basal lung	0.500	0.769	0.550	0.500	1.000
Other	0.140	0.364	0.364	0.140	0.125

NA = not applicable.

thermore, even when using the bolus tracking technique to minimize this problem, the early arterial phase may provide only poor parenchymal contrast in the case of slow circulation (*26*). Nevertheless, it must be acknowledged that, so far, it has not yet been conclusively investigated whether a 30-s delay is superior to the approximately 25-s delay chosen for our study, especially when taking the high variability of vascularity of NET lesions into account.

Interestingly, despite these potential limitations, arterial CT offered the highest interobserver reliability of all CT phases in our analysis, thus also emphasizing the potential of arterial CT to confirm findings observed in other CT subscans. Furthermore, some malignant lesions could be detected only in this phase, and for lesions other than liver metastases, arterial CT was comparable to portal-venous CT in terms of sensitivity and general rating of lesions ($P = 0.9426$–0.9905).

PET was the most sensitive single modality for the detection of lymph node lesions, followed by arterial CT and portal-venous CT. Although the differences in sensitivity between PET and arterial and portal-venous CT were not significant, some malignant lesions were visible exclusively on these scans. Over a quarter (27.5%) of all NET lesions were detected by PET alone, most of these being small PET-positive mesenteric nodules that were considered benign on CT.

In contrast to a study by Ambrosini et al. (*27*), the sensitivity of PET for the detection of bone metastases was low, as can partly be explained by statistical reasons: in our cohort we had only a low total number of osseous metastases combined with a strong patient clustering. Moreover, because a different radiotracer with a different receptor affinity profile was used, only a gross comparison of both SSTR PET studies was possible. However, in concordance with this study, the interobserver reliability for bone lesions was higher for PET ($\kappa = 0.890$) than for CT ($\kappa = 0.495$), because the latter was confronted by a highly variable presentation of bone metastases with a polymorphic picture of osteoblastic, osteolytic, and mixed lesions (*27*).

As demonstrated by the low sensitivity and high interobserver variability, the assessment of pancreatic NET lesions by CT was difficult. In contrast, PET was able to detect all but one of the malignant lesions, resulting in a sensitivity of 94.1% in our patient collective. In a small cohort, Horton et al. reported the best results for arterial CT (*28*). However, this could not be confirmed in the present study, in which the performance of the CT subscans was comparable.

In total, we consider the sensitivities to be realistic in this blinded reading, since false-negatives could be adequately identified by follow-up imaging (e.g., definite metastases on CT/MRI that are SSTR-negative or morphologically unsuggestive lymph nodes that are definitely SSTR-positive).

By contrast, specificities were rather high, as the truth-panel decisions were driven in a high percentage of cases by imaging follow-up using the same criteria for tumor definition as the blinded reading.

In addition, the interpretation of specificity (and sensitivity) was limited in categories with only a low number of total lesions.

In overall performance, PET proved to be the most accurate—and perhaps more important—the most robust imaging submodality. However, anatomic information provided by CT was still required for the correct topographic assignment of a PET-detected focus.

Although portal-venous and venous CT were comparable in sensitivity and thus might potentially be interchangeable, the exclusive detection of lesions by either subscan cannot be ignored. Likewise, in our study arterial CT was the least prominent but most robust of the CT phases—a finding that, in our opinion, makes arterial CT suitable for the verification of lesions detected by other phases.

Concerning PET, we acknowledge that small metastases may be difficult to detect because of partial-volume effects and respiratory motion artifacts (*29*). Moreover, processes such as clonal selection after several lines of therapy could cause some patients to harbor only weakly SSTR-expressing tumor metastases. As a consequence, the overall tumor spread within a patient might be visualized best by using additional PET tracers (e.g., ^{18}F-FDG for NET with a higher proliferation rate) (*30*).

Concerning CT hardware requirements, CT angiography and coronary CT diagnostics, in particular, clearly benefit from 64 or more detector rows (*31*). However, to what extent the resulting high speed of examination is necessary in an oncologic setting has yet to be evaluated. In our opinion, the 16-row CT component met the requirements of the triple-phase protocol in this study quite sufficiently.

Overall, PET and CT performed comparably well in both lesion- and patient-based analysis. In addition, taking all the aforementioned factors for PET and CT imaging into account, it is not surprising that the present study was also able to demonstrate the complementary nature of morphology- and functionality-based imaging of NET (*11*).

CONCLUSION

Triple-phase CT and ^{68}Ga-DOTATOC PET have comparable accuracy in the detection of NET lesions and deliver highly synergistic information. Because additional clinical information is provided by each of the CT subscans, no CT phase can yet be omitted and the triple-phase protocol continues to be strongly recommended in a PET/CT setting.

DISCLOSURE STATEMENT

The costs of publication of this article were defrayed in part by the payment of page charges. Therefore, and solely to indicate this fact, this article is hereby marked “advertisement” in accordance with 18 USC section 1734.

REFERENCES

1. Nissen NN, Kim AS, Yu R, et al. Pancreatic neuroendocrine tumors: presentation, management, and outcomes. *Am Surg.* 2009;75:1025–1029.

2. Yildiz O, Ozguroglu M, Yanmaz T, Turna H, Serdengecti S, Dogusoy G. Gastroenteropancreatic neuroendocrine tumors: 10-year experience in a single center. *Med Oncol.* 2010;27:1050–1056.
3. Makridis C, Oberg K, Juhlin C, et al. Surgical treatment of mid-gut carcinoid tumors. *World J Surg*. 1990;14:377–383
4. Oberg K, Eriksson B. Nuclear medicine in the detection, staging and treatment of gastrointestinal carcinoid tumours. *Best Pract Res Clin Endocrinol Metab.* 2005; 19:265–276.
5. Landry CS, Brock G, Scoggins CR, McMasters KM, Martin RC II. A proposed staging system for small bowel carcinoid tumors based on an analysis of 6,380 patients. *Am J Surg.* 2008;196:896–903.
6. Jonas S, John M, Boese-Landgraf J, et al. Somatostatin receptor subtypes in neuroendocrine tumor cell lines and tumor tissues. *Langenbecks Arch Chir.* 1995;380:90–95.
7. Kwekkeboom DJ, Krenning EP, Scheidhauer K, et al. ENETS Consensus Guidelines for the Standards of Care in Neuroendocrine Tumors: somatostatin receptor imaging with ^{111}In-pentetreotide. *Neuroendocrinology.* 2009;90:184–189.
8. Gabriel M, Decristoforo C, Kendler D, et al. ^{68}Ga-DOTA-Tyr3-octreotide PET in neuroendocrine tumors: comparison with somatostatin receptor scintigraphy and CT. *J Nucl Med.* 2007;48:508–518.
9. Buchmann I, Henze M, Engelbrecht S, et al. Comparison of ^{68}Ga-DOTATOC PET and ^{111}In-DTPAOC (OctreoScan) SPECT in patients with neuroendocrine tumours. *Eur J Nucl Med Mol Imaging.* 2007;34:1617–1626.
10. Khan MU, Khan S, El-Refaie S, Win Z, Rubello D, Al-Nahhas A. Clinical indications for gallium-68 positron emission tomography imaging. *Eur J Surg Oncol.* 2009;35:561–567.
11. Ruf J, Heuck F, Schiefer J, et al. Impact of multiphase ^{68}Ga-DOTATOC-PET/CT on therapy management in patients with neuroendocrine tumors. *Neuroendocrinology.* 2010;91:101–109.
12. Paulson EK, McDermott VG, Keogan MT, DeLong DM, Frederick MG, Nelson RC. Carcinoid metastases to the liver: role of triple-phase helical CT. *Radiology.* 1998;206:143–150.
13. Sundin A, Vullierme MP, Kaltsas G, Plockinger U. ENETS Consensus Guidelines for the Standards of Care in Neuroendocrine Tumors: radiological examinations. *Neuroendocrinology.* 2009;90:167–183.
14. Seemann MD. Detection of metastases from gastrointestinal neuroendocrine tumors: prospective comparison of ^{18}F-TOCA PET, triple-phase CT, and PET/CT. *Technol Cancer Res Treat.* 2007;6:213–220.
15. Zhernosekov KP, Filosofov DV, Baum RP, et al. Processing of generator-produced ^{68}Ga for medical application. *J Nucl Med.* 2007;48:1741–1748.
16. Denecke T, Grieser C, Froling V, et al. Multislice computed tomography using a triple-phase contrast protocol for preoperative assessment of hepatic tumor load in patients with hepatocellular carcinoma before liver transplantation. *Transpl Int.* 2009;22:395–402.
17. Ay MR, Zaidi H. Assessment of errors caused by X-ray scatter and use of contrast medium when using CT-based attenuation correction in PET. *Eur J Nucl Med Mol Imaging.* 2006;33:1301–1313.
18. Prabhakar HB, Sahani DV, Fischman AJ, Mueller PR, Blake MA. Bowel hot spots at PET-CT. *Radiographics.* 2007;27:145–159.
19. Landis JR, Koch GG. The measurement of observer agreement for categorical data. *Biometrics.* 1977;33:159–174.
20. Wieder H, Beer AJ, Poethko T, et al. PET/CT with Gluc-Lys-([^{18}F]FP)-TOCA: correlation between uptake, size and arterial perfusion in somatostatin receptor positive lesions. *Eur J Nucl Med Mol Imaging.* 2008;35:264–271.
21. Kumbasar B, Kamel IR, Tekes A, Eng J, Fishman EK, Wahl RL. Imaging of neuroendocrine tumors: accuracy of helical CT versus SRS. *Abdom Imaging.* 2004;29:696–702.
22. Hartmann H, Zöphel K, Freudenberg R. Radiation exposure of patients during ^{68}Ga-DOTATOC PET/CT examinations [in German]. *Nuklearmedizin.* 2009;48: 201–207
23. Dirix LY, Vermeulen PB, Fierens H, De Schepper B, Corthouts B, Van Oosterom AT. Long-term results of continuous treatment with recombinant interferon-alpha in patients with metastatic carcinoid tumors: an antiangiogenic effect? *Anticancer Drugs.* 1996;7:175–181.
24. Oberg K. Interferon in the management of neuroendocrine GEP-tumors: a review. *Digestion.* 2000;62(suppl 1):92–97.
25. Grozinsky-Glasberg S, Shimon I, Korbonits M, Grossman AB. Somatostatin analogues in the control of neuroendocrine tumours: efficacy and mechanisms. *Endocr Relat Cancer.* 2008;15:701–720.
26. Bae KT. Intravenous contrast medium administration and scan timing at CT: considerations and approaches. *Radiology.* 2010;256:32–61.
27. Ambrosini V, Nanni C, Zompatori M, et al. ^{68}Ga-DOTA-NOC PET/CT in comparison with CT for the detection of bone metastasis in patients with neuroendocrine tumours. *Eur J Nucl Med Mol Imaging.* 2010;37:722–727.
28. Horton KM, Hruban RH, Yeo C, Fishman EK. Multi-detector row CT of pancreatic islet cell tumors. *Radiographics.* 2006;26:453–464.
29. Liu C, Pierce LA II, Alessio AM, Kinahan PE. The impact of respiratory motion on tumor quantification and delineation in static PET/CT imaging. *Phys Med Biol.* 2009;54:7345–7362.
30. Binderup T, Knigge U, Loft A, et al. Functional imaging of neuroendocrine tumors: a head-to-head comparison of somatostatin receptor scintigraphy, ^{123}I-MIBG scintigraphy, and ^{18}F-FDG PET. *J Nucl Med.* 2010;51:704–712.
31. Dewey M, Hoffmann H, Hamm B. CT coronary angiography using 16 and 64 simultaneous detector rows: intraindividual comparison. *Rofo.* 2007;179:581–586.

JNM The Journal of NUCLEAR MEDICINE

^{68}Ga-DOTATOC PET/CT of Neuroendocrine Tumors: Spotlight on the CT Phases of a Triple-Phase Protocol

Juri Ruf, Jan Schiefer, Christian Furth, Ortud Kosiek, Siegfried Kropf, Friederike Heuck, Timm Denecke, Marianne Pavel, Andreas Pascher, Bertram Wiedenmann and Holger Amthauer

J Nucl Med. 2011;52:697-704.
Published online: April 15, 2011.
Doi: 10.2967/jnumed.110.083741

The Journal of Nuclear Medicine is published monthly.
SNMMI | Society of Nuclear Medicine and Molecular Imaging
1850 Samuel Morse Drive, Reston, VA 20190.
(Print ISSN: 0161-5505, Online ISSN: 2159-662X)

SNMMI SOCIETY OF NUCLEAR MEDICINE AND MOLECULAR IMAGING